ISSN 1062-8738, Bulletin of the Russian Academy of Sciences: Physics, 2020, Vol. 84, No. 9, pp. 1126–1130. © Allerton Press, Inc., 2020.
Russian Text © The Author(s), 2020, published in Izvestiya Rossiiskoi Akademii Nauk, Seriya Fizicheskaya, 2020, Vol. 84, No. 9, pp. 1320–1324.

# Magnetic Properties of Fe–Cu–Nb–Si–B Spinning Ribbons

**D. V. Balatskiy[a, b, *], G. S. Kraynova[a], V. S. Plotnikov[a], N. V. Ilin[a], V. V. Tkachev[a], and Yu. V. Knyazev[c]**

[a] *Far Eastern Federal University, Vladivostok, 690950 Russia*

[b] *Institute of Chemistry, Far Eastern Branch, Russian Academy of Sciences, Vladivostok, 690022 Russia*

[c] *Kirensky Institute of Physics, Krasnoyarsk Scientific Center, Siberian Branch, Russian Academy of Sciences, Krasnoyarsk, 660036 Russia*

**e-mail: denis.balatskiy@bk.ru*

Received March 19, 2020; revised April 10, 2020; accepted May 27, 2020

**Abstract**—Dependences of relative saturation magnetization on temperature are measured for amorphous nanocrystalline ribbons of Finemet-type $FeCu_1Nb_3Si_{13.5}B_8$, $FeCu_1Nb_3Si_{13}B_6$, and $FeCu_1Nb_3Si_{13}B_{13}$ compositions. The character of the structural relaxation of amorphous alloys is established by means of Mössbauer spectroscopy, and the main magnetic characteristics are determined. It is found that the structural relaxation of amorphous ribbon proceeds in several stages upon annealing.

**DOI:** 10.3103/S1062873820090063

## INTRODUCTION

Amorphous nanocrystalline materials with controlled fractions of the ordered phase are being studied extensively. One of the most important properties of disordered systems is the presence of magnetic order in the absence of translational symmetry on the atomic level [1, 2]. The properties of amorphous nanocrystalline systems differ from those of both amorphous and crystalline materials [3]. In this regard, nonequilibrium and disordered amorphous and equilibrium amorphous nanocrystalline structures are of great interest [4, 5].

In this work, we investigated amorphous nanocrystalline ribbons of the Finemet-type with different contents of amorphizers of $FeCu_1Nb_3Si_{13.5}B_8$, $FeCu_1Nb_3Si_{13}B_6$, and $FeCu_1Nb_3Si_{13}B_{13}$ compositions ~20 μm thick and produced via spinning (cooling rate, ~$10^6$ K/s).

The dynamics of a ribbon's magnetic properties, its structural stability, and its transition to a crystalline state were monitored while heating from room temperature up to 700°C (heating rate 10 deg/min) using a vibration magnetometer.

The main magnetic characteristics of the samples were determined according to the data on the dependence of the relative saturation magnetization on temperature [5, 6], Curie temperature $T_c^{am}$ of the amorphous state, temperature $T_{cr}$ of the onset of crystallization, the difference between temperatures in the state with zero magnetic moment $\Delta T_{pm}$, temperature $T_{cr}^{max}$ of the maximum magnetic ordering in the crystalline state, and Curie temperature $T_c^{cr}$ of the crystalline state (Table 1).

The Mössbauer spectra were obtained at room temperature in transmission geometry using a $^{57}Co(Rh)$ source. The velocity scale was calibrated using the spectrum of metallic iron (α-Fe). The isomer shifts were determined relative to the center of gravity of the α-Fe spectrum.

The use of Mössbauer spectroscopy enabled us to obtain information on the distribution of magnetic hyperfine fields and the nearest neighbor environment of $^{57}Fe$ atoms for both the initially amorphous samples and ones annealed for 30 min at temperatures of 550 and 650°C (Figs. 1–3). In the initial state, the Mössbauer spectra are those of ferromagnets with wide and

**Table 1.** Characteristic temperatures of $FeCu_1Nb_3Si_{13.5}B_8$, $FeCu_1Nb_3Si_{13}B_6$, and $FeCu_1Nb_3Si_{13}B_{13}$ ribbons

| No. | Composition of sample | $T_C^{am}$, °C | $\Delta T_{pm}$, °C | $T_{cr}$, °C | $T_{cr}^{max}$, °C | $T_c^{cr}$, °C |
|---|---|---|---|---|---|---|
| 1 | $FeCu_1Nb_3Si_{13}B_6$ | 375 | 175 | 550 | 625 | 675 |
| 2 | $FeCu_1Nb_3Si_{13,5}B_8$ | 350 | 200 | 550 | 600 | 650 |
| 3 | $FeCu_1Nb_3Si_{13}B_{13}$ | 400 | 200 | 600 | 625 | 675 |

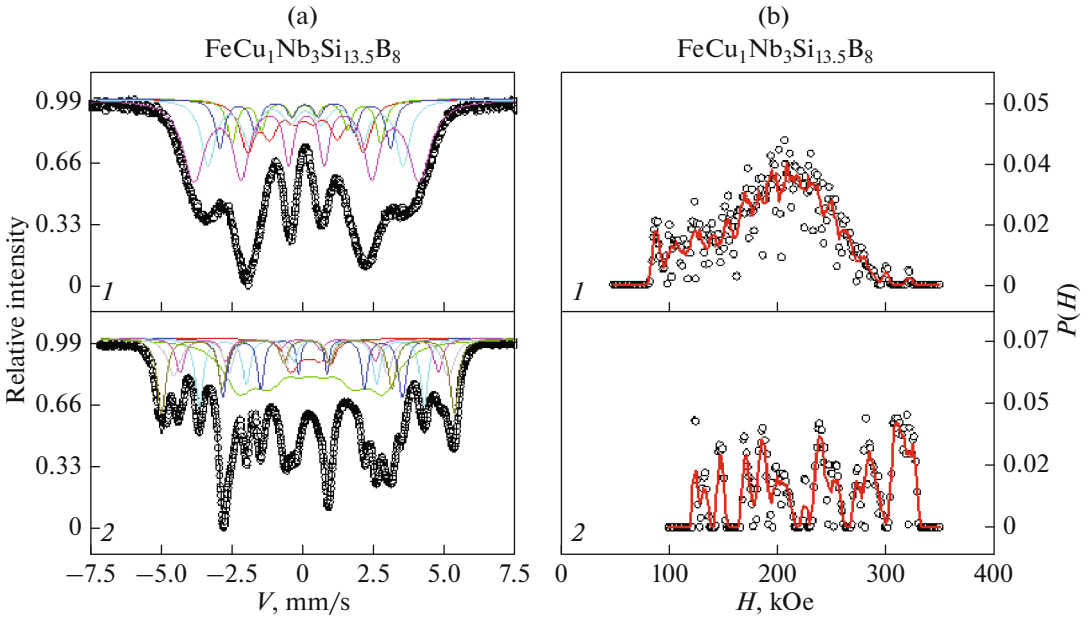


**Fig. 1.** (a) Set of Mössbauer spectra and (b) the distribution of hyperfine magnetic fields in an $FeCu_1Nb_3Si_{13.5}B_8$ ribbon. (*1*) amorphous state, (*2*) sample annealed at 650°C.

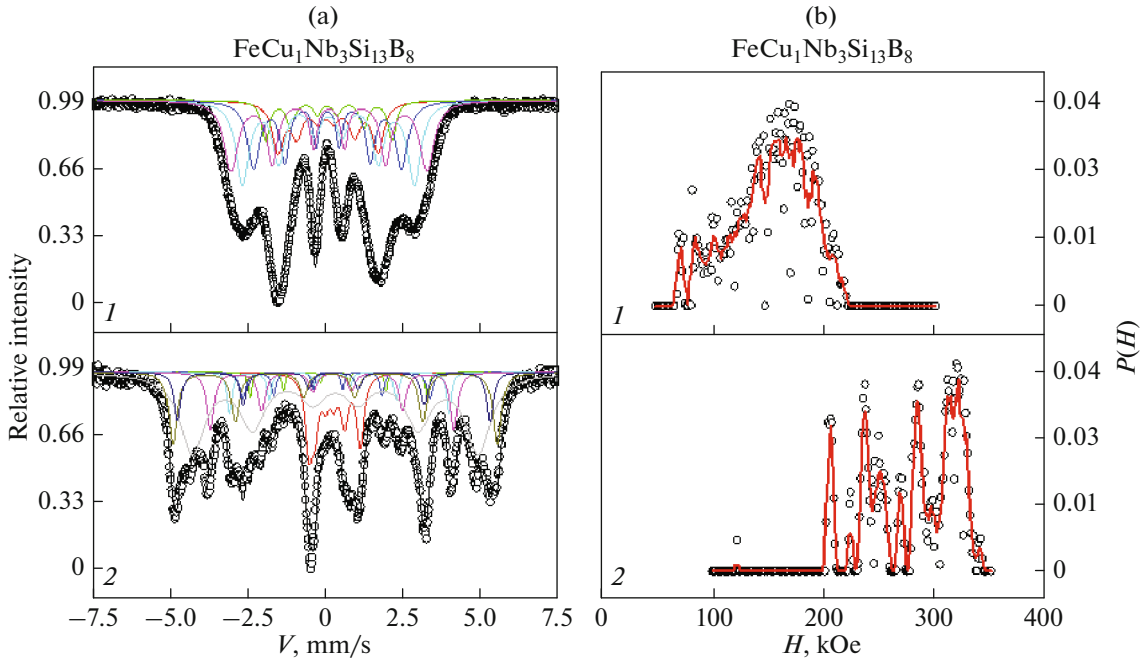


**Fig. 2.** (a) Set of Mössbauer spectra and (b) the distribution of hyperfine magnetic fields in an $FeCu_1Nb_3Si_{13}B_6$ ribbon: (*1*) amorphous state, (*2*) sample annealed at a temperature of 650°C.

overlapping absorption lines corresponding to amorphous materials. Structural relaxation associated with the release of free volume and the removal of rolling tension began as the temperature rose. This was accompanied by the emergence of different crystal phases in the sample that could be identified by means of Mössbauer spectroscopy.

The Mössbauer spectra were processed in two stages. In the first, the distribution of the hyperfine fields in the experimental spectra was determined. The

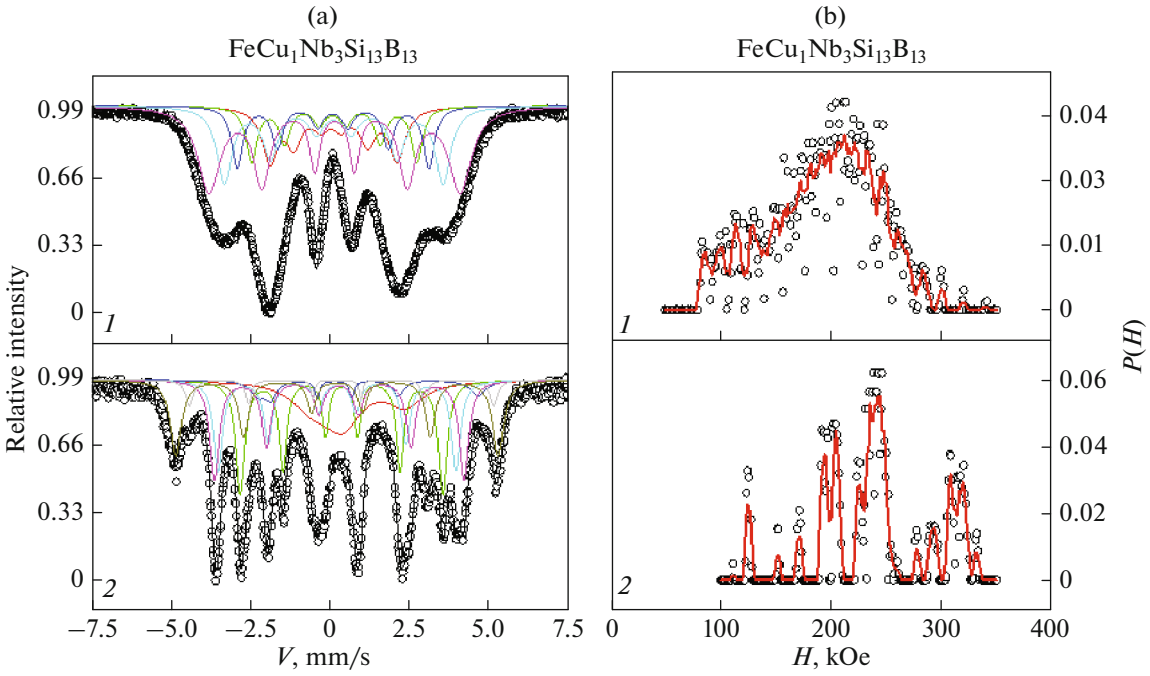


**Fig. 3.** (a) Set of Mossbauer spectra and (b) the distribution of hyperfine magnetic fields in an $FeCu_1Nb_3Si_{13}B_{13}$ ribbon: (*1*) amorphous state, (*2*) sample annealed at 650°C.

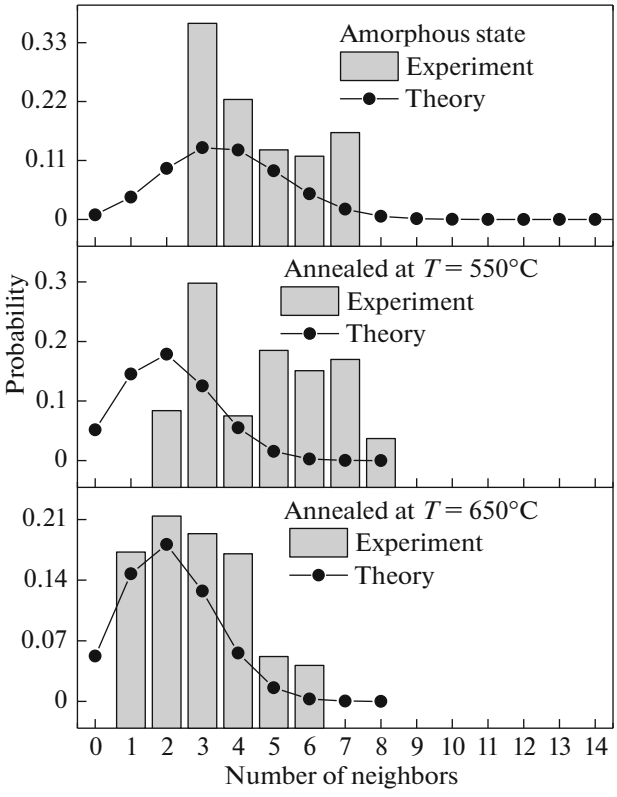


**Fig. 4.** Curve with dots showing the distribution of probabilities of nearest neighbors in the representation of Voronoi polyhedra in the models of RCP structures. Columns show the distribution of the number of impurity atoms *n* in the nearest neighbor environment of iron atoms for an $FeCu_1Nb_3Si_{13}B_{13}$ ribbon.

values of the most probable fields in the studied samples were determined from the distribution of hyperfine fields, which were then introduced into the program to model the theoretical spectrum. The values of the isomeric shift, quadrupolar splitting, and the area and width at the half-height of each subspectrum were varied (Table 2).

Specific features related to the development of probable nonequivalent positions of iron and distortion of its local environment were thus determined. The calculated values of the magnetic fields enabled us to determine the probable positions and nearest neighbor environment of $^{57}Fe$ atoms in the samples (Fig. 4).

With amorphous materials, the central iron atom could have $n = 14$ nearest neighbors and $(14n)$ iron atoms in the nearest environment in the representation of Voronoi polyhedra in models of randomly close-packed structure structures (RCP structures) [1]. The probability of these atomic configurations being present in an amorphous structure was described by the binomial distribution

$$P_n = \frac{0.5}{1-c}\binom{14}{n}(2c)^n(1-2c)^{14-n}, \qquad (1)$$

where $c$ is the concentration of impurity atoms.

The probability of such atomic configurations being present in the crystal structure (i.e., for samples annealed at temperatures of 550 and 650°C) was described by another binomial distribution of the nearest neighbor environment in the representation of

**Table 2.** Parameters for processing the Mössbauer spectra of a $FeCu_1Nb_3Si_{13}B_{13}$ ribbon. *IS* is the isomer shift for α-Fe and the $^{57}Co(Rh)$ source, ±0.005 mm/s; *H* is the hyperfine field, ±5 kOe; *QS* is quadrupolar splitting, ±0.01 mm/s

| | *IS*, mm/s | *H*, kOe | *QS*, mm/s | Relative area, % | Number of neighbors | Phase |
|---|---|---|---|---|---|---|
| Initial | | | | | | |
| S1 | 0.13 | 119.7 | 0.19 | 16.2 | 7 | |
| S2 | 0.16 | 155.6 | 0.12 | 11.8 | 6 | |
| S3 | 0.15 | 180.3 | 0.02 | 13.0 | 5 | |
| S4 | 0.18 | 205.7 | 0 | 22.4 | 4 | |
| S5 | 0.21 | 236.3 | 0 | 36.6 | 3 | |
| Annealed at 550°C | | | | | | |
| S1 | 0 | 113.4 | 1.40 | 4.0 | A8 | Fe–Si |
| S2 | 0.22 | 132.3 | 0 | 17.0 | A7 | |
| S3 | 0.21 | 174.5 | 0.01 | 15.1 | A6 | |
| S4 | 0.33 | 199.5 | 0.08 | 18.4 | A5 | |
| S5 | 0.05 | 205.2 | 0 | 7.3 | A4 | |
| S6 | 0.27 | 245.2 | 0 | 29.8 | A3 | |
| S7 | 0.18 | 310.6 | 0.02 | 8.4 | A2 | |
| Annealed at 650°C | | | | | | |
| S1 | 0.41 | 59.2 | 3.24 | 16.7 | Relax | |
| S2 | 0.14 | 198.4 | 0 | 4.1 | A6 | Fe–Si |
| S3 | 0.46 | 215.1 | 2.13 | 5.2 | A5 | |
| S4 | 0 | 232.8 | 0 | 16.8 | A4 | |
| S5 | 0.06 | 244.3 | 0.04 | 19.1 | A3 | |
| S6 | 0.07 | 297.9 | 0.31 | 21.1 | A2 | |
| S7 | 0 | 315.6 | 0 | 17.0 | A1 | |

a $D0_3$ lattice, in which positions *A* and *D* were determined according to the formula [7]

$$P_n = \frac{0.5}{1-c}\binom{8}{n}(2c)^n(1-2c)^{8-n}. \quad (2)$$

The distribution of probabilities of nearest neighbors in the representation of Voronoi polyhedra in the models of RCP structures and the distribution of the number of impurity atoms *n* in the nearest neighbor environments of iron atoms are shown in Fig. 4.

Positions of iron with nearest neighbor environments of 3 to 7 nonmagnetic neighbors were determined experimentally for the amorphous state (Fig. 4 and Table 2). Positions A2–A8 related to the Fe–Si phase were determined for a sample annealed at a temperature of 550°C. Positions A1–A6 were determined for a sample annealed at a temperature of 650°C. The nearest neighbor environment for the samples annealed at 650°C corresponded to a theoretical dependence calculated using a binomial distribution. This is explained by the temperature of 650°C being the one at which structural relaxation was observed in the studied samples up to crystallization.

## CONCLUSIONS

Thermomagnetic studies of rapidly quenched Fe–Cu–Nb–Si–B alloys showed that an increase in the percentage of metalloids (Si, B) with no change in the concentration of alloying additives (Cu, Nb) raised temperature $T_c^{am}$ of the magnetic phase transition in the paramagnetic state, reduced temperature interval $\Delta T_{pm}$ of the paramagnetic state, and increased temperature $T_{cr}$ of crystallization.

Mössbauer spectroscopy data enabled us to obtain the distribution of hyperfine fields, the most probable value of which was ~210 kOe for amorphous rapidly quenched alloys with metalloid contents of more than

20%; $H_{st}$ ~210 kOe for the $FeCu_1Nb_3Si_{13}B_6$ alloy; and $H_{st}$ ~180 kOe for the $FeCu_1Nb_3Si_{14}B_5$ alloy. The above values of hyperfine fields corresponded to nearest neighbor environments of iron atoms that range from 3 to 7 nonmagnetic neighbors. The increase in the most probable $H_{st}$ is mirrored in the number of nonmagnetic atoms falling from 5 to 1.

Annealing to temperatures of 550 and 650°C revealed scenarios of the structural relaxation of alloys according to the change in the distribution of hyperfine fields and the number of nonmagnetic atoms in the nearest neighbor environment. The increased dispersion of the $H_{st}$ distribution and the probabilities of the nearest neighbors allowed us to present the Mössbauer spectra as a superposition of 7–8 subspectra, which mirrored the complex character of the structure of rapidly quenched alloys at this stage of structural relaxation.

## REFERENCES

1. Handrich, K. and Kobe, S., *Amorphe Ferro- und Ferrimagnetika* (Amorphous Ferro- and Ferrimagnetics), Berlin: Akademie, 1980.
2. Suzuki, K., Fujimori, H., and Hashimoto, K., *Amorphous Metals*, London: Butterworths, 1982.
3. Glezer, A.M. and Shurygina, N.A., *Amorfno-nanokristallicheskie splavy* (Amorphous-Nanocrystalline Alloys), Moscow: Fizmatlit, 2013.
4. Chunling, Q., Qingfeng, H., Yongyan, L., et al., *Mater. Sci. Eng., A*, vol. 69, p. 513.
5. Tkachev, V.V., Tsesarskaya, A.K., Ilin, N.V., et al., *AIP Conf. Proc.*, 2017, vol. 1874, 040051.
6. Ilin, N.V., Tkachev, V.V., Fedorets, A.N., et al., *Bull. Russ. Acad. Sci.: Phys*, 2018, vol. 82, no. 7, p. 860.
7. Rixeckeret, G., Schaaf, P., and Gonser, U., *Phys. Status Solidi A*, 1993, vol. 139, p. 309.

*Translated by D. Marinin*